CORRECTION OF FLUTTER BOUNDARY OF NON-PLANAR WING USING MEASURED LOCAL MACH NUMBER

Atsushi Kanda*, Takashi Kai*
*Japan Aerospace Exploration Agency

Abstract

This research shows flutter boundary corrections of a reentry space vehicle with a non-planar wing. For anti-symmetric mode flutter boundaries of the reentry space vehicle model, numerical predictions using the doublet-point method (DPM) were different from experimental results in a part of a low supersonic region. The cause of the discrepancy is thought to be a local flow over the wing differing from the free stream.

Flutter boundary analyses are therefore corrected by using revised Mach numbers on the basis of measured local Mach numbers in the transonic wind tunnel of Japan Aerospace Exploration Agency (JAXA). In the case of revised Mach numbers calculated by local Mach numbers at places of large mode displacement on the wing, the corrected numerical results show good agreement with experimental ones. Therefore it is confirmed that correction using local Mach numbers improves the accuracy of flutter boundary predictions.

1 Introduction

The reentry space vehicle HOPE project had been proceeding in Japan (Fig.1). One of the vehicle characteristics was a wing shape at the beginning of the project, which was a non-planar wing called as the 'tip-fin' configuration. This vehicle was planned to be launched by the H-IIA, which was Japanese original rocket, return to the Earth (free flight).

In a free flight, an anti-symmetric mode flutter becomes critical like conventional aircraft. However, in anti-symmetrical flutter speeds of the tip fin-shaped reentry space vehicle model, numerical predictions using the doublet-point method (DPM) [1] and p-k method were considerably different from experimental results in a low supersonic region.

On the other hand, during launch by H-IIA rocket, the configuration is different from conventional aircraft as shown in Fig.2. The vehicle has also an anti-symmetric mode flutter which is caused by roll elasticity in spite of non-free-flight. This flutter is due to an elastic attachment between the vehicle and the rocket. In this configuration, similarly, analytical flutter speeds were largely different from the experiments in a supersonic region.

The cause of these discrepancies is thought to be the local flow over the wing differing from the free stream. In other words, a local Mach number is thought to be different from a Mach number of the free stream. There may be a striking difference, especially in the case of the non-planar wing. A wind tunnel model with a rigid wing has been made to measure local Mach numbers. At first, local total and local static pressures have been measured using Pitot tubes and pressure sensors respectively in a transonic wind tunnel. Next, local Mach numbers in a supersonic region are calculated using measured pressures. Shockwaves in a supersonic region are taken into consideration here. Flutter boundary is reevaluated by using corrected Mach numbers on the basis of measured local Mach numbers.
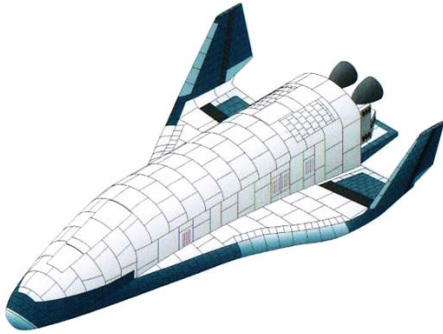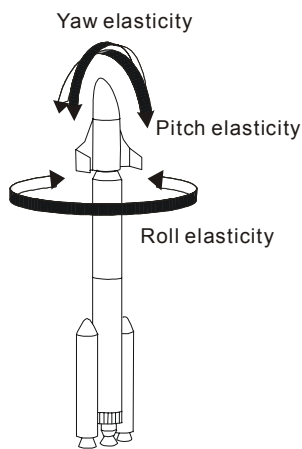
Fig.1 HOPE

Fig.2 Launching Configuration of HOPE

2 Wind Tunnel Model

The wind tunnel model installed in the wind tunnel is shown in Fig.3. The rigid wing, which is made of the aluminum alloy 7075-T651, is consisted of a main part and a tip-fin part. Each part is NACA0010 airfoil. The wing shape is same as the model in which numerical flutter boundaries were different from experimental those.

The fuselage of this wind tunnel model is the length of 677mm, both of the height and the width of 160mm. The main part of the wing has 200mm in span, 400mm in chord length at the root and 120mm at the tip. There are kinks on the leading and trailing edges at the location of 80mm in span. The tip-fin part has the cant angles of 14 degrees, the span length of 120mm, and the chord length of 60mm at the tip.
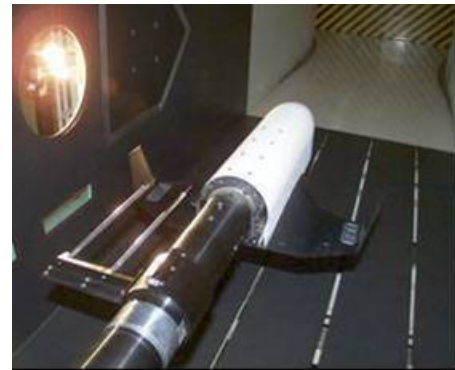

Fig.3 Wind Tunnel Model

3 Measurement

This section describes a method to obtain local Mach numbers. Local Mach numbers are calculated by using local static pressures and total pressures measured in experiments. Experimental results in the transonic wind tunnel of JAXA are also shown.

3.1 Static Pressure

Shown in Fig.4, four pressure sensors (absolute pressure transducer Kulite XCS-062-15A) are installed to measure static pressures in the right wing. Two inboard sensors ch1, ch2 are located at the span of 45.5mm from the wing root and at the chord of 31.1%, 90.7%, respectively. Two outboard sensors ch3, ch4 are at the span of 140.5mm and at the chord of 31.1%, 81.5%.
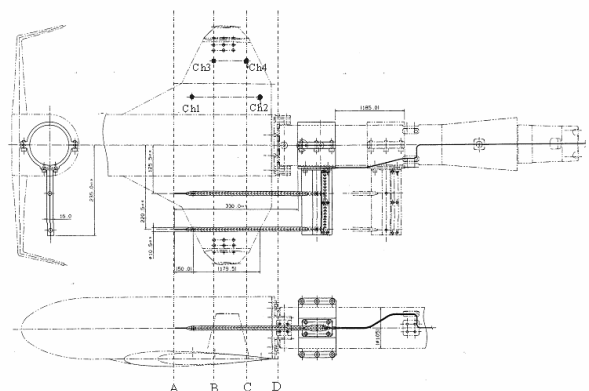

Fig.4 Pressure Sensors and Pitot Tubes

3.2 Total Pressure

Local total pressures are measured by two Pitot tubes which are located nearby the left wing and quartz manometers. The Pitot tubes are set at the left wing to avoid interactions with pressure sensors in the right wing. Spanwise positions of the Pitot tubes are collocated to static pressure sensor positions and are respectively located at the span of 45.5mm and 140.5mm. These tubes can be manually traversed along an axis of the model. By using this function, local total pressures are measured at the position of A (120mm aft from the wing root), B (246mm), C (336mm), D (424mm) as shown in Fig.4.

Total and static pressures are measured in a steady flow condition with Mach numbers of 0.6, 0.8, 1.0, 1.1, 1.2, 1.3 and 1.4. Total pressures P_0 in a plenum chamber are 80k and 100kPa.

3.3 Local Mach Number

A method to calculate local Mach numbers from measured static and total pressures is shown here. Assuming an isentropic steady flow, the relationship of a total pressure P_0, a static pressure P and a Mach number M is following.

$$\frac{P}{P_0} = \left(\frac{1}{1+(\gamma-1)M^2/2} \right)^{\frac{\gamma}{\gamma-1}} \quad (1)$$

where γ is the specific heat ratio.

Note that shockwave occurs in front of Pitot tube in a supersonic region as shown in Fig.5. In a supersonic region, total pressures are measured as P_{02} behind shockwaves caused by Pitot tubes. Therefore, a Pitot tube gives a total pressure inside a shockwave. Equation (1) is valid at outside and inside of shockwave, respectively. The conservation of mass, momentum and enthalpy of the flow leads

$$\frac{P_2}{P_1} = \frac{1+\gamma M_1^2}{1+\gamma M_2^2} \quad (2)$$

$$M_2^2 = \frac{(\gamma-1)M_1^2/2+1}{\gamma M_1^2-(\gamma-1)/2} \quad (3)$$

where subscript 1 and 2 mean outside and inside of a shockwave. Substituting Eq.(3) into Eq.(2) becomes

$$\frac{P_2}{P_1} = \frac{2\gamma}{\gamma+1}M_1^2 - \frac{\gamma-1}{\gamma+1} \quad (4)$$

A relationship between the local Mach number M_1, P_1 and P_{02} is given by Eq.(5) which is based on the Rankine-Hugoniot relation.

$$\frac{P_1}{P_{02}} = \frac{P_1}{P_2}\frac{P_2}{P_{02}} = \frac{\left(\frac{2\gamma}{\gamma+1}M_1^2 - \frac{\gamma-1}{\gamma+1} \right)^{\frac{1}{\gamma-1}}}{\left(\frac{\gamma+1}{2}M_1^2 \right)^{\frac{\gamma}{\gamma-1}}} \quad (5)$$

The local Mach number M_1 is calculated by solving Eq.(5) with the regula-falsi method from measured P_1 and P_{02} in a supersonic region. On the other hand, the local Mach number for a subsonic region is simply calculated by Eq.(6) from Eq.(1).

$$M = \sqrt{\frac{2}{\gamma-1}\left\{ \left(\frac{P}{P_0} \right)^{\frac{1-\gamma}{\gamma}} - 1 \right\}} \quad (6)$$
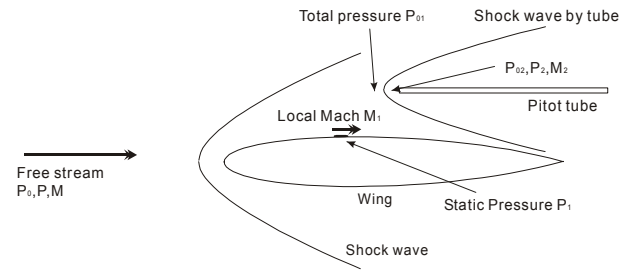

Fig.5 Schematic of Supersonic Flow

Local Mach numbers are distributed quantities over the wing. In this case, the local Mach number can be obtained at each pressure sensor location. Figure 6 shows measured local Mach numbers. It is clear that local Mach numbers are higher than free stream Mach numbers.
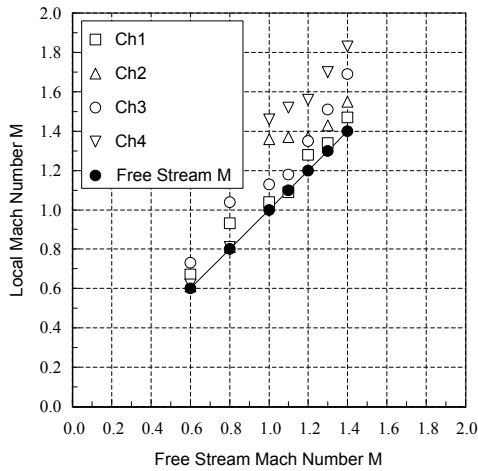
Fig.6 Local Mach Number

4 Correction of Flutter Boundary

There are two cases in which the experimental flutter boundaries were different from analytical those in a lower supersonic region. One is the anti-symmetric mode flutter in a free flight configuration. The other is the anti-symmetric mode flutter in a launching configuration. This section shows a method to correct flutter boundary using measured local Mach numbers and correction results.

4.1 Correction Method

The local mach number M_l is obtained at each location of pressure sensors. However, representative Mach number is required for the flutter analysis based on the linear lifting surface theory like the DPM or the doublet-lattice method (DLM). The flutter is coupling of the 3rd and 5th natural vibration modes where the deflection is larger in the outboard wing than inboard. Therefore, the local flow over the outboard wing has larger effects on the unsteady aerodynamics. One of the methods to obtain representative Mach number is to employ an average of local Mach numbers at two pressure sensors in the outboard wing. Here, the corrected Mach number M' as representative is given by

$$M' = \left(M_{ch3} + M_{ch4} \right)/2 \qquad (7)$$

The Second method is to employ an average of all four local Mach numbers. The corrected Mach number M'' is given by

$$M' = \left(M_{ch1} + M_{ch2} + M_{ch3} + M_{ch4} \right)/4 \quad (8)$$

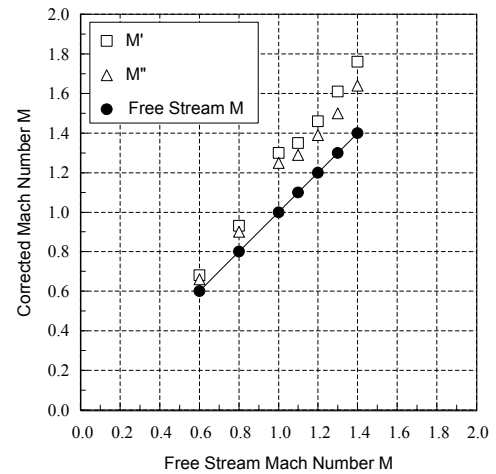The corrected Mach number M' and M'' is shown in Fig.7.

Fig.7 Corrected Mach Number

4.2 Flutter in Free Flight Configuration

The anti-symmetric mode flutter of the reentry space vehicle model (Fig.7) became critical in a free flight configuration. This flutter was coupling of the anti-symmetric bending mode and the anti-symmetric torsional mode of the wing. In subsonic region, analyses had good agreements with experimental results with flutter boundaries. However, flutter boundaries of experiments were significantly higher than analyses at $M = 1.1$ and 1.2 (see [2]).

Fig.7 Free Flight Model

Flutter analyses are conducted by using corrected Mach numbers. Flutter boundaries are calculated by the p-k method with the structural damping of 0.03. The results are shown in Fig.8.

U_F means the non-dimensional flutter speed without correction, while U_F' and U_F'' respectively means corrected non-dimensional flutter speed by M' and M''. Note that the non-dimensional flutter speed is defined by Eq.(9), assuming inviscid, irrotational and isentropic.

$$\overline{U_F} = \frac{1}{2\pi f_\alpha b}\sqrt{\frac{\pi b S_w}{2m}}\sqrt{\frac{\gamma P_0 M^2}{1+(\gamma-1)M^2/2}} \qquad (9)$$

where m is the wing mass, b is a half chord of the main wing at the root, S_w is the wing area, f_α is the natural frequency of the torsional mode and γ is the specific heat ratio.
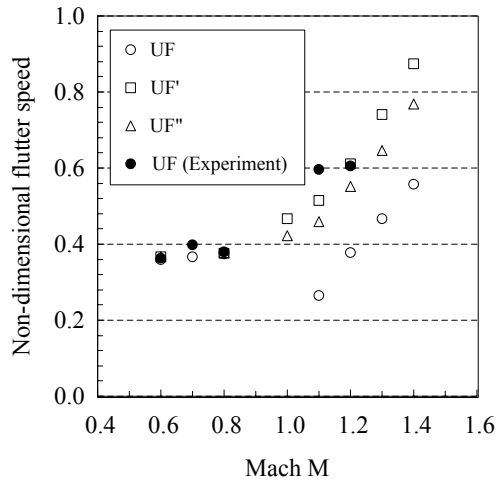

Fig.8 Corrected Flutter Boundaries in Free Flight

4.3 Flutter in Launching Configuration

The wind tunnel model with an elastic roll support for a launching configuration is shown in Fig.9. In this configuration, it was shown that the elastic roll mode by the attachment between the vehicle and the rocket affected to the anti-symmetric mode flutter. The similar discrepancy occurred in this flutter in the lower supersonic region [3][4].

Fig.9 Launching Configuration Model

Similarly, flutter analyses are conducted by using corrected Mach numbers. The results are shown in Fig.10.
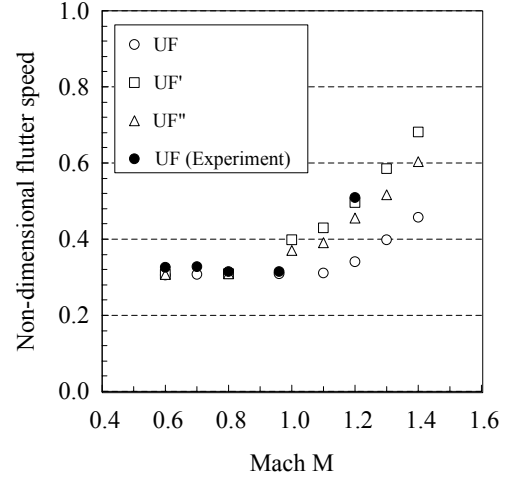

Fig.10 Corrected Flutter Boundaries in Launching

4.4 Discussion

The analyses of the non-dimensional flutter speed U_F were much different from experiments for both of the free flight and the launching model in a low supersonic region. However, the correction of Mach numbers makes the difference small. Especially, U_F' have good agreements with experiments. It can be also shown that there are no effects of the correction in a subsonic region. Therefore, the corrected flutter analysis is consistent over all Mach numbers.

5 Conclusion

Flutter boundaries have been corrected by using measured local Mach number. As a result, flutter boundaries of the analyses become close to experimental ones. Using corrected Mach numbers at locations where the deflection of the wing is larger, especially, analyses have good agreements with experiments. It is also shown that the DPM can conduct higher accuracy of flutter boundaries by using corrected Mach numbers. Therefore, the local Mach number has to be taken into account for flutter analyses of a non-planar wing like a tip-fin configuration.

References

[1] Ueda, T.: Unsteady Aerodynamic Calculations for General Configurations by the Doublet-Point Method, *Technical Report of National Aerospace Laboratory*, TR-1101T, 1991.

[2] Kanda, A. and Ueda, T.: Anti-Symmetric Mode Flutter of Winged Reentry Space Vehicle, *Technical Report of National Aerospace Laboratory*, TR-1342, 1997 (in Japanese).

[3] Kanda, A. and Ueda, T.: Effects of Rolling Elasticity on Flutter Characteristics at Launching Configuration of Re-entry Winged Space Vehicle, *Technical Report of National Aerospace Laboratory*, TR-1380, 1999 (in Japanese).

[4] Kanda, A. and Ueda, T.: Flutter of Winged Reentry Space Vehicles Affected by an Elastic Attachment in Launching Configuration, *Transaction of the Japan Society for Aeronautical and Space Sciences*, Vol.46, No.154, 2004.